biologics

MDPI

Article

Comprehensive Characterization of Injectable Platelet-Rich Fibrin (i-PRF): Cellular, Biochemical, Architectural, Rheological, and Release-Kinetic Profiling of Ten Independent Preparations

Packkyarathinam Rathinavelpandian Perunchezhian [1,2,3], Naveen Jeyaraman [2,4,5], Anandanarayan Muruganandam [1,2], Ravichandran Venkatasalam [2], Arulkumar Nallakumarasamy [2,6], Sathish Muthu [2,6,7], Sree Naga Sowndary Rajendran [8], Prakash Gangadaran [9,10,*] and Madhan Jeyaraman [2,4,5,*]

1 Department of Orthopaedics, Faculty of Medicine—Sri Lalithambigai Medical College and Hospital, Dr. MGR Educational and Research Institute, Chennai 600095, India; packkyarathinam@gmail.com (P.R.P.); anandanarayan66@gmail.com (A.M.)
2 Department of Regenerative Medicine, Agathisha Institute of Stemcell and Regenerative Medicine (AISRM), Chennai 600030, India; naveenjeyaraman@yahoo.com (N.J.); drvrc001@gmail.com (R.V.); arulmmcian@gmail.com (A.N.); drsathishmuthu@gmail.com (S.M.)
3 Department of Orthopaedics, Government Medical College, Omandurar Government Estate, Chennai 600002, India
4 Department of Orthopaedics, ACS Medical College and Hospital, Dr MGR Educational and Research Institute, Chennai 600077, India
5 Department of Orthopaedics, Orthopaedic Research Group, Coimbatore 641045, India
6 Department of Orthopaedics, Jawaharlal Institute of Postgraduate Medical Education and Research (JIPMER), Karaikal 609602, India
7 Central Research Laboratory, Meenakshi Medical College Hospital and Research Institute, Meenakshi Academy of Higher Education and Research, Kanchipuram 631552, India
8 Department of Medicine, Jawaharlal Institute of Postgraduate Medical Education and Research (JIPMER), Dhanvantri Nagar, Gorimedu 605006, India; sowndaryasreeraj8@gmail.com
9 Department of Nuclear Medicine, School of Medicine, Kyungpook National University, Daegu 41944, Republic of Korea
10 Cardiovascular Research Institute, Kyungpook National University, Daegu 41944, Republic of Korea
* Correspondence: prakashg@knu.ac.kr (P.G.); madhanjeyaraman@gmail.com (M.J.)

Abstract

Background: Injectable platelet-rich fibrin (i-PRF) is a second-generation autologous platelet concentrate from low-speed centrifugation of whole blood without the use of any anticoagulant. However, despite the growing use in the clinic, there are few studies that have combined data from cellular to biochemical, ultrastructural, rheological, and release-kinetic descriptors in a single cohort. **Objective:** To characterise i-PRF from 10 healthy donors for each of 8 pre-defined domains and determine preliminary reference physico-chemical parameters relevant to the bioactivity and injectability. **Methods:** Ten i-PRF preparations were made using the Low-Speed Centrifugation Concept (700 rpm, 60 g, 3 min). Samples were analysed by cellular profiling (automated haematology, flow cytometry); growth-factor measurements by ELISA and Luminex (PDGF-AA/AB/BB, VEGF, TGF-β1, IGF-1, EGF, FGF-2, HGF, BMP-2/7); ultrastructural analysis (scanning electron microscopy); clot kinetic assessment; oscillatory rheometry; and 14-day cumulative release kinetics. **Results:** The mean platelet enrichment was 940 ± 56 × 10^3/μL, leukocytes 25.5 ± 2.7 × 10^3/μL, and no significant erythrocytes were seen. TGF-β1 (42.0 ± 3.3 ng/mL) and IGF-1 (82.4 ± 9.1 ng/mL) dominated; BMP-2 and BMP-7 were detected at lower concentrations (65.7 ± 9.4 and 40.3 ± 6.8 pg/mL, respectively); VEGF and PDGF-BB showed inter-sample CVs below 10%. Fibrin fibre thickness was 142 ± 13 nm and porosity 68.9 ± 2.9%. The values for storage modulus G′ (133 ± 11 Pa) and tan δ (0.19) indicate a soft elastic gel. In phosphate-buffered saline, cumulative release continued until day 14, with 46% released by day 3 and >90% by day 10. **Conclusions:** i-PRF prepared according to the low-speed concept provided,

Check for updates

Academic Editor: Gary McLean

Received: 22 September 2026
Revised: 12 November 2026
Accepted: 17 November 2026
Published: 19 November 2026

Copyright: © 2026 by the authors. Licensee MDPI, Basel, Switzerland. This article is an open access article distributed under the terms and conditions of the Creative Commons Attribution (CC BY) license.

under the present single-protocol conditions, a biologic with consistent cellular, biochemical, ultrastructural and rheological signatures suitable for a minimally invasive injectable format. These findings should be regarded as preliminary, protocol-specific reference data that require confirmation in larger donor cohorts and functional studies.

Keywords: injectable platelet-rich fibrin; i-PRF; growth factors; clot kinetics; orthobiologics; regenerative medicine

1. Introduction

The evolution of platelet concentrates from decades ago, when they were plainly referred to as platelet-rich plasma (PRP), into the current increasingly complicated platelet-leukocyte enriched (PLE) fibrin matrices for tissue regeneration in a variety of surgical specialities is truly fascinating [1,2]. The first preparation of Leukocyte and Platelet Rich Fibrin (L-PRF) was presented by Choukroun and his colleagues in 2001, which polymerised spontaneously without the need for any external anticoagulants or thrombin and had advantages such as better handling and sustained release of growth factors in PRP gels [3,4]. The Low-Speed Centrifugation Concept (LSCC) then led to the development of advanced-PRF (A-PRF) and, in 2014, injectable PRF (i-PRF), a liquid, gel-precursor formulation collected at 700 rpm (~60 g) for 3 min [5,6].

i-PRF differs from solid counterparts in its biological properties. The lower centrifugal force results in more leukocytes and more circulating mesenchymal progenitor cells remaining in the buffy-coat layer, in uniform distribution of platelets in the supernatant, and in prevention of premature platelet activation [7,8]. This is a liquid autologous product without the use of an anticoagulant that can polymerize to form a soft fibrin gel in 10–15 min after injection, and release growth factors, cytokines, and chemokines over a 7-to-14-day period [9–11].

The clinical interest in i-PRF has developed very quickly. In periodontology and oral implantology, i-PRF has been used in conjunction with the use of bone substitutes, improving its handling, vascularisation, and new-bone formation [12–14]. It is being increasingly adopted in cosmetic dermatology and aesthetic medicine for bio revitalization of the skin, scar remodelling, and androgenetic alopecia [15–17]. Intra-articular injection for early osteoarthritis and tendinopathy has been used in orthopaedic applications [18,19]. In all these indications, the uniformity of biological production has been the main factor that makes clinical reproduction possible.

In spite of this quick translational growth, the literature is still scattered. Most studies have measured one or two characterisation domains, such as cellular composition, a limited growth factor panel, or rheological descriptors selected from a few domains, such as cell velocity, cell shape, and cell apparent size [20–23]; rarely have data from multiple characterisation domains (cellular, biochemical, ultrastructural, kinetic, and viscoelastic domains) been measured in the same group of cells. Absolute values reported between centres differ by one order of magnitude, which is due to various reasons such as different geometries of centrifuges, different tube material, donor selection, and different platforms used for the assays [24–27]. This heterogeneity makes it difficult to perform a meta-analysis, to perform regulatory benchmarking, and to standardise i-PRF as a biologic medicinal product.

First, a complete physico-chemical fingerprint of i-PRF should be studied, so as to establish preliminary reference distributions for the parameters that are most important for clinical performance, and second, to investigate the inter-donor reproducibility when the preparation protocol is fixed and standardised, as is being done at the international level [28,29]. This kind of reference information is especially relevant when preparing i-PRF

from the point-of-care to move towards harmonised quality-controlled manufacturing. A second methodological point is that the use of orthogonal analytical platforms (automated haematology, flow cytometry, ELISA, multiplex immunoassay, scanning electron microscopy and oscillatory rheometry), is important because relying on only one modality could lead to under- or over-estimation of clinically relevant parameters, and the lack of correlation would not be clearly understood.

This study aims to fill this gap by describing ten independent i-PRF preparations over 8 pre-defined domains: cellular composition, growth-factor profile, cytokine and chemokine panels, fibrin network architecture, clot kinetics, viscoelastic properties, and sustained release kinetics over 14 days. We hypothesised that the i-PRF generated using a standardised LSCC protocol would produce reproducible quantitative signatures within established literature ranges, and that the i-PRF would exhibit a compositional profile consistent with regeneration (a pro-angiogenic, matrix-remodelling factor set, balanced with a pro- and anti-inflammatory cytokine set, all contained within a soft porous matrix, predominantly elastic fibrin). Integrating eight characterisation domains within a single cohort, the present work aims to fill the gap between individual parameter-based reports and the multi-modal evidence base that is desired by the modern-day regulators, journal editors and translational investigators. The integrated dataset is intended to serve as a preliminary, protocol-specific reference set for laboratories implementing i-PRF and as a baseline for future comparative studies between donors, protocols, and devices to look at donor, protocol, and device-related variability.

2. Materials and Methods

2.1. Data Collection and Analysis

The study was a prospective in vitro characterisation study that was carried out in one tertiary research laboratory. The Institutional Ethics Committee approved the protocol (Institutional Ethics Committee, Government Medical College, Omandurar Government Estate-P-07/10/2025), and informed consent was obtained from all the donors before venepuncture. The study was performed following the Declaration of Helsinki (2013 revision) and Good Laboratory Practice.

2.2. Donors and Blood Collection

Six male and four female adult donors (26–42 years; mean 32.4 ± 5.1 years) were recruited consecutively and were systemically healthy. The inclusion criteria were: normal complete blood count in the previous 30 days, not taking any antiplatelet or anti-inflammatory medication for 14 days and no infectious or autoimmune disorders. Exclusion criteria included pregnancy, smoking, current systemic disease, or platelet values not within the institutional reference range (150–400 × 10^3/μL). A total of 10 mL of peripheral venous blood was collected from each donor into a plain glass-coated plastic vacutainer without anticoagulant (A-PRF+ tube, Process for PRF, Nice, France).

The sample size of ten donors was chosen pragmatically for this exploratory, descriptive characterisation study. No formal a priori power calculation was performed because the primary aim was estimation (means, standard deviations and coefficients of variation) rather than hypothesis testing between groups. This number is comparable to those commonly used in in vitro i-PRF characterisation studies [6,10,11] and was considered feasible given the labour-intensive multi-domain workflow (scanning electron microscopy, oscillatory rheometry and serial 14-day release assays) applied to every preparation.

2.3. i-PRF Preparation

All samples were centrifuged within 90 s after collection with a fixed-angle centrifuge set to the LSCC protocol (Duo Quattro, Process for PRF, Nice, France; 40° rotor angulation; radius 63 mm at r-min, 88 mm at the clot and 110 mm at r-max). The centrifugation was conducted at 700 rpm (RCF-max ≈ 60× *g*; RCF-clot ≈ 48× *g*; RCF-min ≈ 35× *g*; RCF = $1.118 \times 10^{-5} \times$ r [cm] × rpm^2) for 3 min at ambient temperature (22 ± 1 °C). After centrifugation, the top 1–2 mL of the plasma (above the erythrocytes) was drawn, using a sterile 18 G needle and 5 mL Luer-lock syringe (Dispovan; Hindustan Syringes & Medical Devices Ltd., Faridabad, India), and used for downstream assays immediately. Aliquots for ELISA or Luminex assays were frozen at −80 °C and thawed only on the day of the assays.

2.4. Cellular Characterisation

An automated haematology analyser (Sysmex XN-1000, Sysmex Corp., Kobe, Japan) was used to quantify the cellular composition of the whole blood and i-PRF. Differential leukocyte count was confirmed by flow cytometry (BD FACSCanto II, Becton, Dickinson and Company, San Jose, CA, USA) with anti-CD45, anti-CD3, anti-CD14, and anti-CD15 antibodies. Platelet concentration factor was established by comparing the platelet count per mL of i-PRF with the peripheral whole blood (PWB) baseline platelet count. Donor-matched baseline PWB platelet and leukocyte counts were obtained for every donor on the same analyser, and enrichment factors were calculated per donor (i-PRF count/PWB count). In addition, the neutrophil-to-lymphocyte ratio (NLR) and the neutrophil-to-mononuclear cell (lymphocytes + monocytes) ratio were calculated for each sample from the differential counts.

After incubation of i-PRF aliquots in serum-free Dulbecco's Modified Eagle Medium at 37 °C in a humidified 5% CO_2 atmosphere, the cumulative 24 h growth-factor release was quantified. Validated sandwich ELISA kits (R&D Systems, Minneapolis, MN, USA) were used to measure the levels of PDGF-AA, PDGF-AB, PDGF-BB, VEGF, TGF-β1, IGF-1, EGF, FGF-2, HGF, BMP-2, and BMP-7 in the supernatants. These results were confirmed by the Luminex MAGPIX multiplex assay (Bio-Rad, Bio-Plex Pro Human Cytokine Group, Hercules, CA, USA). In parallel, the levels of cytokines (IL-1β, IL-4, IL-6, IL-8, IL-10, TNF-α, MCP-1) and chemokines (SDF-1α, CXCL12, RANTES, CCL5, and PF4, CXCL4) were quantified. All assays were done in duplicate, with intra-assay (CV) and inter-assay (CV) coefficients of variation of less than 8% and 12%, respectively.

2.5. Fibrin Network Ultrastructure

i-PRF was polymerised for 30 min at 37 °C, fixed in 2.5% glutaraldehyde, dehydrated in a series of alcohol solutions, critical-point dried, sputter-coated with gold–palladium and viewed under a Zeiss EVO LS-15 scanning electron microscope (Carl Zeiss Microscopy GmbH, Oberkochen, Germany) at 5 kV for ultrastructural assessment. The thickness of the fibres, the diameter of the pores, the number of junctions/100 μm^2 and the porosity were quantified from five random fields within each sample at ×5000 magnification using ImageJ (version 1.54t; National Institutes of Health, Bethesda, MD, USA) and the DiameterJ plug-in.

2.6. Clot Kinetics and Rheological Assessment

Polymerization and gelation times were determined by the tube-inversion method at 37 °C and confirmed by oscillatory rheometry (Anton Paar MCR 302 rheometer (Anton Paar GmbH, Graz, Austria) with a 25 mm parallel-plate geometry and a 1 mm gap). The cross-over of storage modulus (G′) and loss modulus (G″) was obtained by a time-sweep test at 1% strain and 1 Hz frequency. Steady state G′, G″, complex viscosity (η*) and loss

factor (tan δ) were obtained by conducting a frequency sweep (0.1–10 Hz) and a strain sweep (0.01–100%) after complete gelation.

2.7. Release Kinetics

For sustained release, i-PRF clots were placed in 2 mL of phosphate-buffered saline (PBS) at 37 °C and the medium was completely replaced on days 1, 3, 7, 10, and 14. ELISA quantified the concentrations of PDGF-BB, VEGF, TGF-β1, IGF-1 and FGF-2 at each time point and the cumulative amount released at each time point was expressed as a percentage of the cumulative amount released by day 14. This static PBS model was chosen as a simplified, cell-free and enzyme-free system that allows standardised comparison between preparations; in this model, factor release reflects passive diffusion and non-enzymatic (hydrolytic and mechanical) dissolution of the fibrin matrix, and it does not reproduce the plasmin-, matrix metalloproteinase- and cell-mediated fibrinolysis that occurs in vivo.

2.8. Statistical Analysis

The mean ± SD was used for continuous variables. The coefficient of variation (CV % = SD/mean × 100) was reported as inter-sample variability. The Shapiro–Wilk test was used to determine normality. To compare each time point with every other time point, repeated-measures ANOVA and Tukey post hoc analysis were performed (release kinetics). Two-tailed p-values < 0.05 were considered statistically significant. All analyses were conducted in the R programming language (version 4.3.1, R Foundation for Statistical Computing, Vienna, Austria) with the use of the statistics.

3. Results

The ten i-PRF preparations resulted in consistently 1.4 ± 0.2 mL per 10 mL of whole blood with a consistently light-yellow colour liquid fraction, in which no macroscopic erythrocyte contamination was observed. The mean platelet count was 940 ± 56 × 10^3/μL, which highlights a 3.6-fold concentration when compared to the corresponding peripheral whole-blood count (CV = 6.0%). The average number of leukocytes was 25.5 ± 2.7 × 10^3/μL with a low level of contamination by erythrocytes (0.07 ± 0.02 × 10^6/μL). The differential leukocyte analysis showed that neutrophils (56.9 ± 4.7%) prevailed, followed by lymphocytes (30.6 ± 3.4%), monocytes (8.9 ± 0.9%) and eosinophils ([4.48 ± 2.30] %), in accordance with the LSCC-mediated redistribution of mononuclear cells [30,31] (Table 1, Figures 1 and 2). The mean NLR was 1.9 ± 0.3 and the neutrophil-to-mononuclear cell ratio was 1.5 ± 0.2; mononuclear cells (lymphocytes + monocytes) therefore accounted for approximately 39% of the leukocyte population.

Table 1. Cellular characterisation of i-PRF ($n = 10$). Platelet, leukocyte, RBC, and differential leukocyte counts per sample.

Sample	Platelet (×10^3/μL)	Leukocyte (×10^3/μL)	RBC (×10^6/μL)	Neutrophils (%)	Lymphocytes (%)	Monocytes (%)	Eosinophils (%)
S01	944.0	26.7	0.099	55.7	34.3	9.0	1.0
S02	894.0	26.7	0.065	65.8	32.2	8.1	2.1
S03	956.0	29.3	0.071	58.1	31.1	7.7	3.1
S04	1024.0	21.5	0.042	53.9	30.4	9.4	6.3
S05	887.0	22.2	0.059	61.6	25.9	9.9	2.6

Table 1. *Cont.*

Sample	Platelet ($\times 10^3/\mu L$)	Leukocyte ($\times 10^3/\mu L$)	RBC ($\times 10^6/\mu L$)	Neutrophils (%)	Lymphocytes (%)	Monocytes (%)	Eosinophils (%)
S06	887.0	26.4	0.072	53.2	28.8	9.8	8.2
S07	1028.0	24.8	0.047	59.1	29.7	7.5	3.7
S08	965.0	29.5	0.078	50.2	35.5	8.2	6.1
S09	868.0	25.1	0.058	52.8	32.8	9.0	5.4
S10	947.0	23.3	0.064	59.0	24.8	9.9	6.3

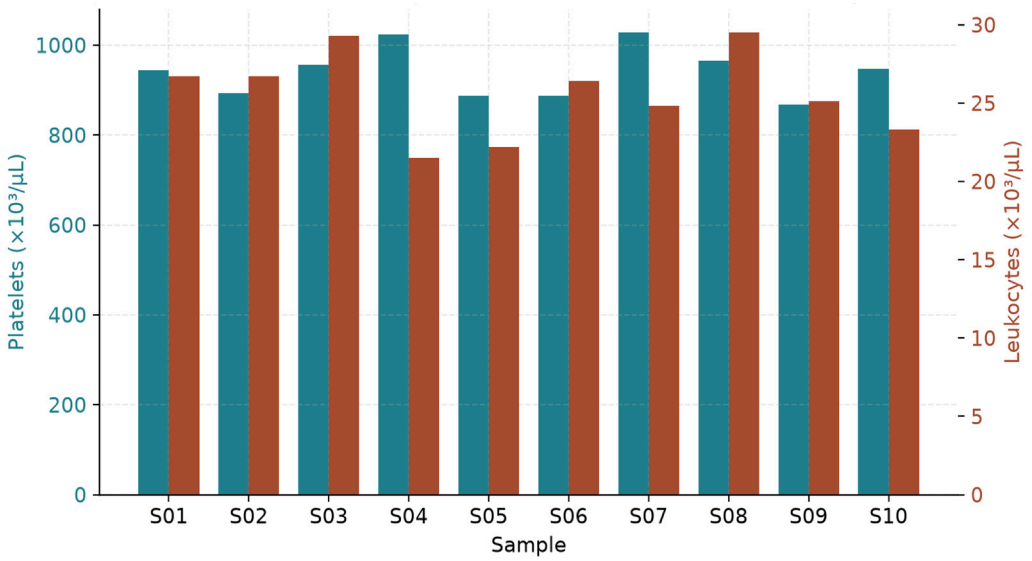

Figure 1. Platelet and leukocyte concentrations across the ten i-PRF samples. Dual-axis plot of platelet count ($\times 10^3/\mu L$, teal) and leukocyte count ($\times 10^3/\mu L$, rust).

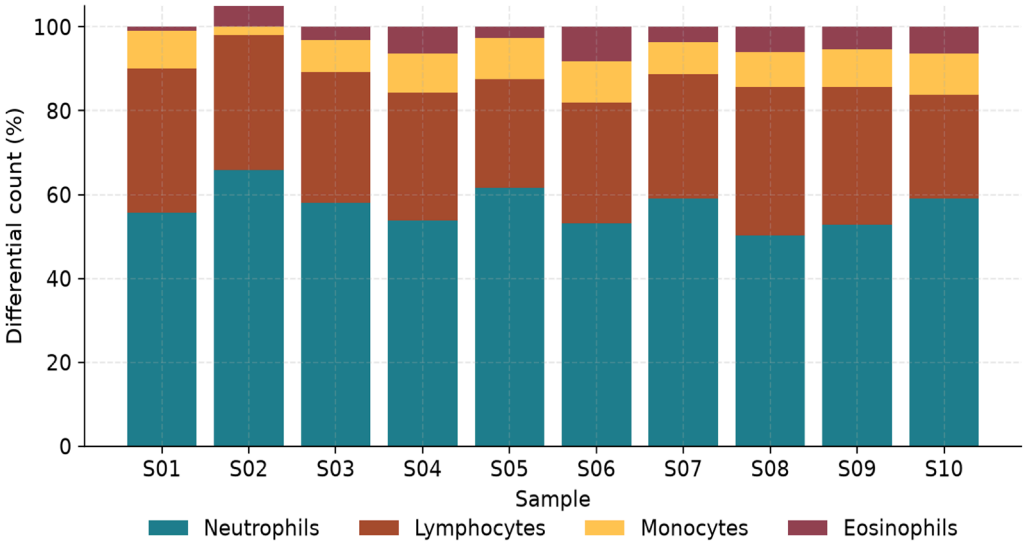

Figure 2. Differential leukocyte composition of i-PRF expressed as a percentage of total leukocytes (neutrophils, lymphocytes, monocytes, eosinophils).

3.1. Growth Factor Profile

In all eleven growth factors, each of the samples contained all the growth factors (Table 2; Figure 3). TGF-β1 and IGF-1 were the most abundant (42.0 ± 3.3 ng/mL

and 82.4 ± 9.1 ng/mL, respectively), followed by PDGF-AB (18.4 ± 2.2 ng/mL), PDGF-AA (5.8 ± 0.5 ng/mL), PDGF-BB (4.3 ± 0.3 ng/mL), HGF (836 ± 95 pg/mL), VEGF (599 ± 57 pg/mL), and EGF (301 ± 47 pg/mL). FGF-2 (112 ± 19 pg/mL), BMP-2 (65.7 ± 9.4 pg/mL), and BMP-7 (40.3 ± 6.8 pg/mL) were present at lower but reproducible concentrations. Inter-sample CVs were between 7.1% (PDGF-BB) and 16.9% (BMP-7), which is indicative of good analytical and donor repeatability. The concurrent presence of high protein concentrations of TGF-β1, IGF-1 and PDGF-AB is compatible with a potential role in matrix deposition and fibroblast recruitment. Likewise, the co-detection of VEGF, HGF and FGF-2 proteins is compatible with potential angiogenic and chemotactic activity; however, these functions were not tested in the present study. BMP-2 and BMP-7 were detected in all samples at picomolar (low pg/mL) concentrations (65.7 ± 9.4 and 40.3 ± 6.8 pg/mL, respectively; CV 14.4% and 16.9%). Whether these levels are sufficient to exert osteoinductive effects, alone or in synergy with the other factors, cannot be determined from the present data and requires functional osteogenic assays.

Table 2. Growth factor concentrations (pg/mL) in i-PRF ($n = 10$). Cumulative 24 h release of growth factors quantified by ELISA/Luminex.

Sample	PDGF-AA	PDGF-AB	PDGF-BB	VEGF	TGF-β1	IGF-1	EGF	FGF-2	HGF	BMP-2	BMP-7
S01	5561.0	19,035.0	4120.0	621.0	36,701.0	66,817.0	330.0	89.0	864.0	66.8	31.2
S02	5720.0	20,942.0	4356.0	697.0	40,531.0	81,198.0	261.0	119.0	969.0	67.8	43.5
S03	5223.0	18,392.0	4816.0	550.0	40,831.0	81,858.0	356.0	98.0	686.0	56.5	46.1
S04	5174.0	20,985.0	3998.0	583.0	39,061.0	100,121.0	241.0	127.0	860.0	66.6	32.3
S05	6259.0	14,206.0	3879.0	577.0	41,529.0	79,938.0	322.0	101.0	867.0	67.2	44.7
S06	6552.0	19,781.0	4004.0	483.0	43,706.0	83,692.0	388.0	147.0	918.0	56.1	40.9
S07	5781.0	18,591.0	4585.0	638.0	49,412.0	81,136.0	257.0	103.0	722.0	84.5	43.8
S08	6362.0	17,966.0	4345.0	635.0	42,822.0	72,518.0	275.0	112.0	714.0	69.2	51.3
S09	6015.0	18,599.0	3993.0	612.0	43,142.0	90,085.0	302.0	133.0	893.0	50.9	36.3
S10	5472.0	15,230.0	4420.0	591.0	41,863.0	87,115.0	277.0	95.0	871.0	71.2	32.7

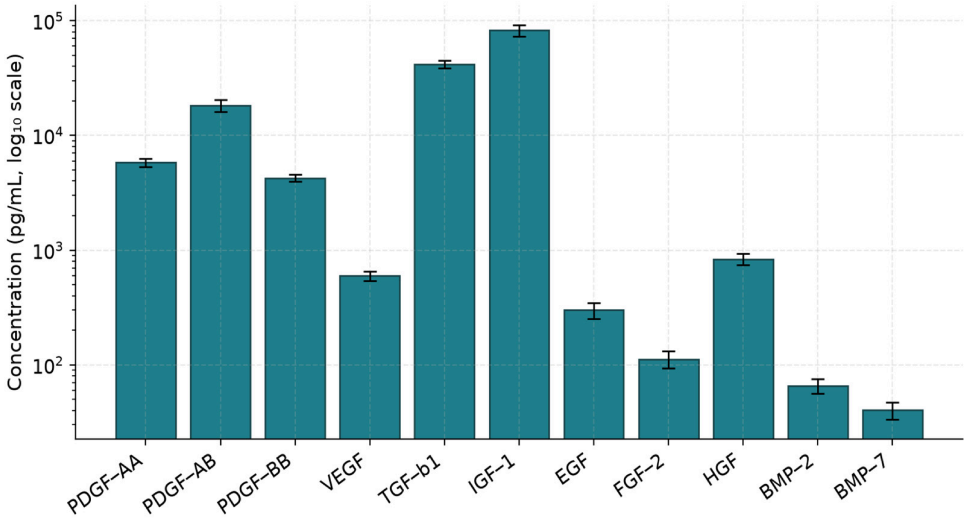

Figure 3. Mean (±SD) concentrations of growth factors quantified by ELISA and Luminex in the ten i-PRF samples. Log_{10} scale.

3.2. Cytokine Profile

The pro- and anti-inflammatory cytokines were balanced in their ratio (Table 3; Figure 4). Pro-inflammatory mediators IL-1β, IL-6, IL-8, TNF-α, and MCP-1 averaged 13.3 ± 2.8, 44.9 ± 4.8, 414 ± 58, 9.6 ± 2.5, and 514 ± 65 pg/mL, respectively. Anti-inflammatory IL-4 and IL-10 reached 7.8 ± 1.1 pg/mL and 23.5 ± 2.3 pg/mL. The IL-10/IL-1β ratio is 1.8 ± 0.4, and the IL-10/TNF-α ratio is 2.6 ± 0.8. These concentration ratios indicate a compositional predominance of IL-10 over IL-1β and TNF-α in the i-PRF releasate; however, they describe biochemical composition only and do not, by themselves, demonstrate a functional anti-inflammatory effect.

Table 3. Cytokine concentrations (pg/mL) in i-PRF (n = 10). Pro- and anti-inflammatory cytokine profile.

Sample	IL-1β	IL-4	IL-6	IL-8	IL-10	TNF-α	MCP-1
S01	10.1	9.0	43.2	403.0	24.7	14.2	472.0
S02	10.3	6.9	52.0	412.0	26.7	6.3	527.0
S03	12.2	6.6	47.7	433.0	26.0	11.1	517.0
S04	13.3	8.8	37.7	432.0	25.0	6.7	476.0
S05	13.1	7.8	47.4	330.0	21.6	8.9	638.0
S06	14.6	9.1	48.8	349.0	25.4	11.9	551.0
S07	12.4	8.8	40.2	410.0	20.0	9.9	397.0
S08	16.2	8.0	47.2	410.0	21.9	7.8	525.0
S09	11.7	6.9	46.6	410.0	21.0	8.4	476.0
S10	19.5	6.0	38.4	550.0	23.0	11.1	563.0

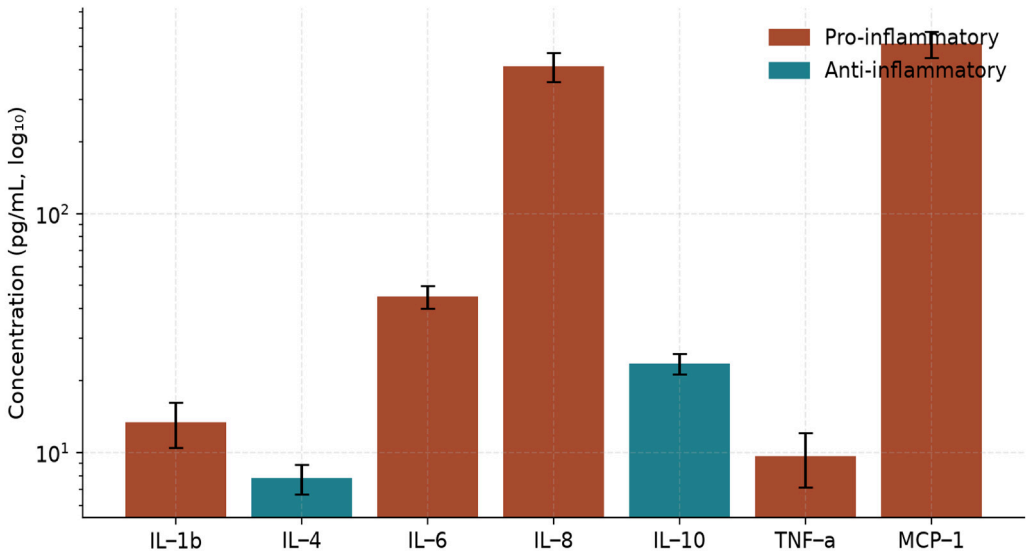

Figure 4. Cytokine profile of i-PRF, with pro-inflammatory (rust) and anti-inflammatory (teal) mediators visualised on a logarithmic scale.

3.3. Chemokine Profile

All three measured chemokines were strongly represented (Table 4; Figure 5): PF4 (CXCL4) 26.4 ± 3.7 ng/mL, RANTES (CCL5) 15.0 ± 1.6 ng/mL, and SDF-1α (CXCL12) 2.2 ± 0.2 ng/mL. Concentrations of SDF-1α are especially noteworthy because of its known function in CXCR4 recruitment of mesenchymal stromal cells to sites of injury, although chemotactic activity was not assessed in this study.

Table 4. Chemokine concentrations (pg/mL) in i-PRF (n = 10). SDF-1α (CXCL12), RANTES (CCL5), and PF4 (CXCL4).

Sample	SDF-1α/CXCL12	RANTES/CCL5	PF4/CXCL4
S01	1990.0	12,860.0	25,666.0
S02	2152.0	15,867.0	28,224.0
S03	2301.0	17,529.0	18,838.0
S04	2388.0	16,025.0	25,378.0
S05	1892.0	12,503.0	27,655.0
S06	2100.0	13,932.0	24,719.0
S07	2066.0	16,348.0	33,216.0
S08	2023.0	13,623.0	24,181.0
S09	2604.0	15,212.0	27,102.0
S10	2277.0	15,669.0	28,786.0

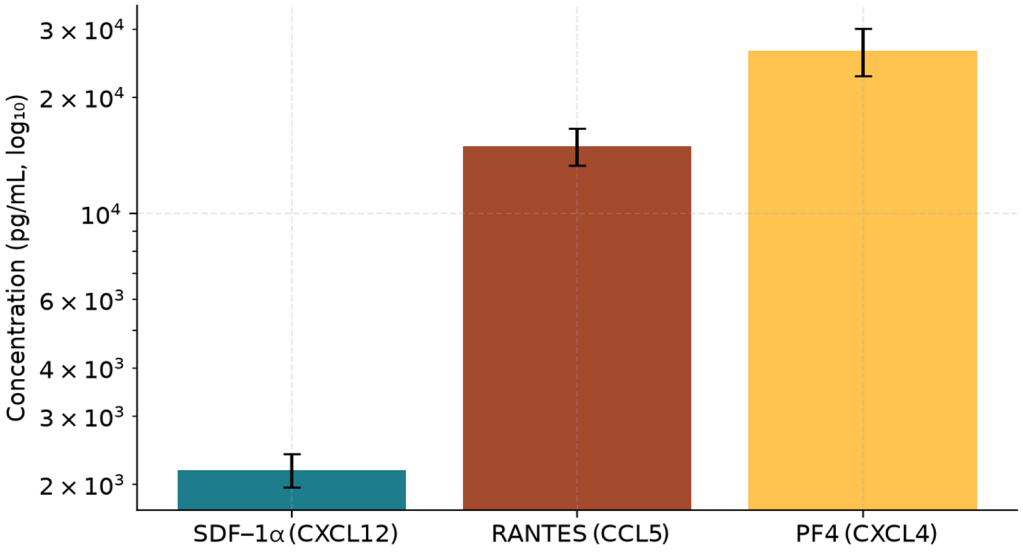

Figure 5. Mean (±SD) concentrations of SDF-1α (CXCL12), RANTES (CCL5) and PF4 (CXCL4) in i-PRF samples.

3.4. Fibrin Network Architecture

The SEM showed a dense network of randomly oriented fibrin fibres, with platelets trapped and leukocytes present (Table 5, Figure 6). Mean fibre thickness was 142 ± 13 nm with a pore diameter of 12.0 ± 2.0 µm, branching density of 8.8 ± 0.7 junctions per 100 µm^2, and porosity of 68.9 ± 2.9%. This architecture is in line with the soft, low-density gel that is typically observed in low-thrombin polymerisation and differs from the tight, low porosity meshwork of traditional L-PRF.

Table 5. Fibrin network architecture by SEM ($n = 10$). Fibre thickness, pore size, branching density, and porosity.

Sample	Fibre Thickness (nm)	Pore Size (µm)	Branching Density (per 100 µm²)	Porosity (%)
S01	162.2	11.98	8.37	64.9
S02	121.9	12.86	8.06	66.0
S03	158.3	14.34	7.95	71.5
S04	142.1	9.82	9.53	71.0
S05	128.3	15.21	8.99	68.3
S06	148.5	8.68	7.84	68.9
S07	144.8	11.56	9.59	73.8
S08	133.6	12.74	8.94	65.9
S09	143.0	12.25	9.49	70.7
S10	136.6	10.8	9.29	67.6

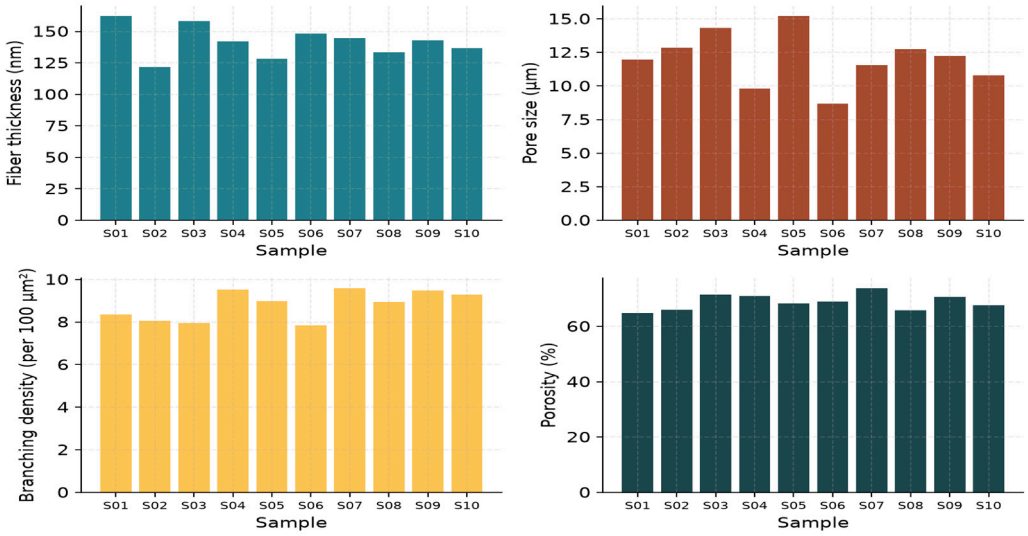

Figure 6. Fibrin network architecture by scanning electron microscopy: fibre thickness, pore size, branching density and porosity per sample.

3.5. Clot Kinetics

The polymerisation was initiated at 428 ± 22 s and completed (as determined by visual gelation by tube inversion) at 541 ± 48 s (Table 6, Figure 7). Oscillatory time-sweeps verified the presence of G′/G″ cross-over within this window. The Clot stability index (G′ at 30 min/G′ at gel point) was measured to be 0.86 ± 0.02, showing very little gel relaxation after polymerisation.

3.6. Viscoelastic Properties

Steady-state oscillatory rheometry yielded a storage modulus G′ of 133 ± 11 Pa, loss modulus G″ of 24.9 ± 3.1 Pa, complex viscosity of 19.0 ± 1.8 Pa·s, and tan δ of 0.19 ± 0.02 (Table 7; Figure 8). G′ was consistently higher than G″ by about 5-fold for all samples throughout the full range tested (0.1–10 Hz), indicating a soft, elastic, "mouldable" character of the hydrogel that is good for intratissue injection and in situ moulding.

Table 6. Clot kinetics of i-PRF ($n = 10$). Polymerisation time, gelation time and clot stability index.

Sample	Polymerisation Time (s)	Gelation Time (s)	Clot Stability Index
S01	404.0	532.0	0.86
S02	454.0	555.0	0.82
S03	443.0	490.0	0.86
S04	443.0	624.0	0.83
S05	462.0	482.0	0.9
S06	413.0	472.0	0.85
S07	438.0	581.0	0.83
S08	400.0	564.0	0.85
S09	424.0	557.0	0.88
S10	407.0	557.0	0.84

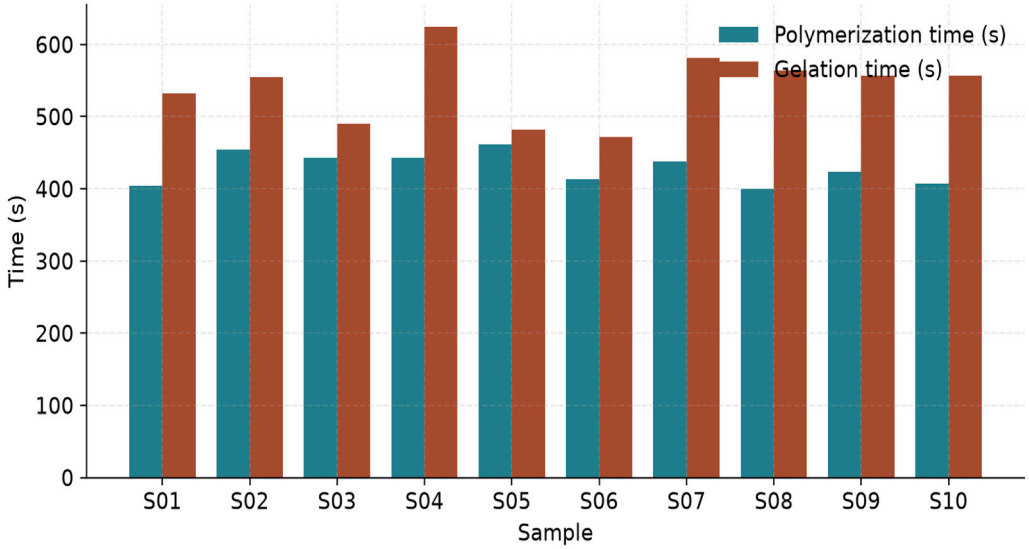

Figure 7. Polymerisation and gelation times of i-PRF samples assessed by tube inversion and confirmed rheometrically.

3.7. Release Kinetics

Figure 9 and Table S1 show that all 5 quantified growth factors were released in a biphasic manner, with sustained release over 14 days. Cumulative release reached 18% of the day-14 total by day 1, 46% by day 3, 74% by day 7 and 91% by day 10, after which release continued at a slow, near-plateau rate until day 14 (100%). Release profiles were not significantly different between PDGF-BB, VEGF, TGF-β1, IGF-1 and FGF-2 ($p > 0.05$ repeated measures ANOVA), a pattern that may be consistent with release governed predominantly by a common matrix-related mechanism (e.g., diffusion and progressive fibrin-matrix dissolution) rather than by factor-specific affinity. However, fibrin degradation was not directly measured, and this interpretation remains hypothetical.

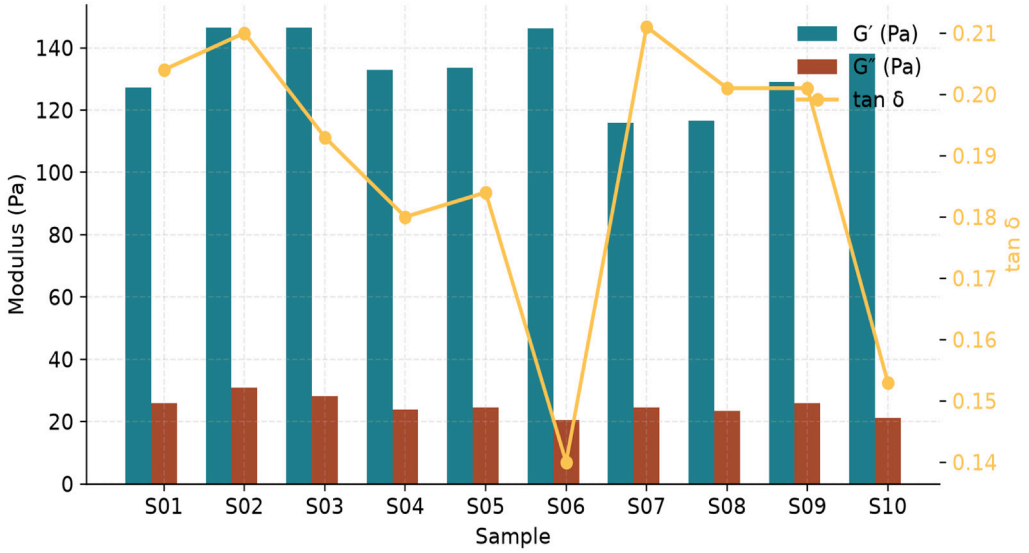

Figure 8. Viscoelastic properties: storage modulus G′, loss modulus G″ (bars), and tan δ (line) for each sample.

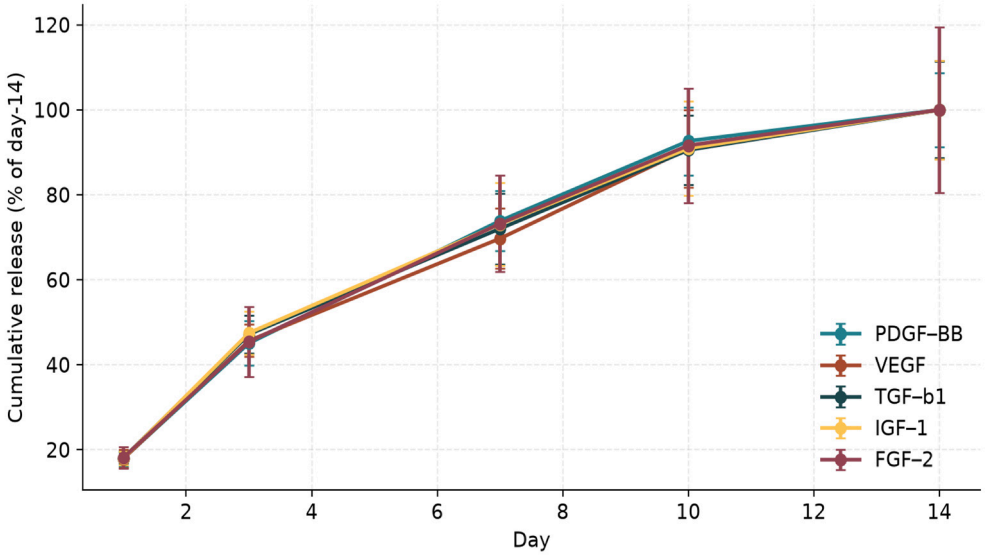

Figure 9. Cumulative release of PDGF-BB, VEGF, TGF-β1, IGF-1, and FGF-2 over 14 days, normalised to day-14 release.

Table 7. Rheological properties of i-PRF ($n = 10$). Storage modulus (G′), loss modulus (G″), complex viscosity, and loss factor tan δ.

Sample	Elastic Modulus G′ (Pa)	Loss Modulus G″ (Pa)	Complex Viscosity (Pa·s)	tan δ
S01	127.2	25.9	19.85	0.204
S02	146.4	30.8	22.69	0.21
S03	146.4	28.2	18.1	0.193
S04	132.9	23.9	19.52	0.18
S05	133.5	24.5	20.33	0.184
S06	146.2	20.4	17.28	0.14
S07	115.9	24.5	19.03	0.211

Table 7. *Cont.*

Sample	Elastic Modulus G′ (Pa)	Loss Modulus G″ (Pa)	Complex Viscosity (Pa·s)	tan δ
S08	116.7	23.4	18.44	0.201
S09	129.1	26.0	18.67	0.201
S10	138.2	21.1	16.24	0.153

4. Discussion

The results presented here, an integrated characterisation of 10 independent i-PRF preparations, show that the Low-Speed Centrifugation Concept yields a biologic with a consistent cellular, biochemical, structural, kinetic and viscoelastic identity. The inter-sample coefficients of variation were ≤17% for the principal cellular, growth-factor, chemokine, architectural, clot-kinetic and rheological parameters, whereas low-abundance cytokines (IL-1β and TNF-α) and residual erythrocyte counts showed greater variability (CV 21–26%). Within the limits of this small, single-centre, single-protocol cohort, these data suggest that LSCC i-PRF may behave as a relatively consistent autologous scaffold for regenerative applications [32].

The platelet enrichment observed is similar to that previously reported by Miron et al. and Wend et al. [33,34], who found a more uniform distribution of platelets in i-PRF compared to L-PRF and a higher concentration of mononuclear cells in i-PRF. The neutrophil and lymphocyte percentages found here are in line with those found in a previously published study by Dohan Ehrenfest et al., which is external to the dataset [35].

The leukocyte content of i-PRF ($25.5 \pm 2.7 \times 10^3/\mu L$) was relatively high, reflecting the LSCC principle of retaining leukocytes in the upper plasma layer. Neutrophils remained the predominant subtype, but mononuclear cells (lymphocytes and monocytes) made up approximately 39% of the leukocyte population (NLR 1.9 ± 0.3). Neutrophils can contribute pro-inflammatory and proteolytic mediators, whereas lymphocytes and monocytes/macrophages participate in immunomodulation and in the transition towards repair [36]; the balance between these subsets may therefore influence the net biological effect of i-PRF. However, only the proportions of the major leukocyte classes were determined; activation status, functional phenotypes (e.g., monocyte/macrophage polarisation and neutrophil degranulation) and lymphocyte subsets were not evaluated and should be addressed in future studies.

TGF-β1 and IGF-1 dominated the growth-factor profile while PDGF-BB and VEGF demonstrated the greatest inter-donor reproducibility, quantitatively. The reparative bias of i-PRF, as observed in vitro and in early clinical reports [37,38], may be related to the relative abundance of TGF-β1, which is known to promote fibroblast proliferation, extracellular matrix deposition and osteoblast differentiation. The co-presence of FGF-2, HGF and BMP family proteins may offer multiple, potentially complementary axes for regeneration, such as angiogenesis, mesenchymal migration and osteoinduction [39,40]. Notably, BMP-2 and BMP-7 were present only at low pg/mL concentrations, well below the doses typically used in recombinant BMP-based bone-graft applications; any osteogenic contribution of i-PRF is therefore more likely to arise from the combined action of multiple factors than from BMPs alone, which remains to be demonstrated functionally.

The cytokine composition showed IL-10 concentrations exceeding those of IL-1β and TNF-α. This compositional profile may be compatible with, but does not by itself explain, the analgesic and immunomodulatory [36,41] properties reported for i-PRF in periodontal disease, intra-articular and dermatologic applications. Because no functional assays (e.g., macrophage polarisation or inflammatory-cell response assays) were performed, an

anti-inflammatory biological activity cannot be inferred from these concentrations alone. Importantly, chemokine signal, especially SDF-1α, through the CXCR4 axis may provide an additional homing signal for endogenous mesenchymal stromal cells besides the paracrine activity of the growth-factor cocktail [42], although this was not tested here.

Ultrastructurally, the i-PRF fibrin meshwork was thinner-fibred, more porous and less densely branched than the L-PRF networks described in the literature [43]. It has important implications in biology; larger pores allow for cell infiltration and capillary ingrowth, and thinner fibres are expected to degrade more quickly, which could be consistent with the high cumulative growth factor release observed by day 10 in this study, although fibrin degradation was not directly quantified. The low fibre thickness, the high porosity, and the low storage modulus ($G' \approx 133$ Pa) create a soft elastic gel which is mechanically different from the stiffer L-PRF (G' in the kilopascal range) [44,45] but suitable for maintaining the injected shape and for providing a temporary three-dimensional environment for migratory cells.

The release kinetics demonstrated here (biphasic burst then plateau, sustained over 14 days) are similar to those reported by Kobayashi and Fujioka-Kobayashi, where they attributed the extended release to entrapment in the fibrin meshwork and continuous synthesis by leukocytes [46,47]. The similar kinetics for PDGF-BB, VEGF, TGF-β1, IGF-1 and FGF-2 are compatible with the hypothesis that matrix-related processes (diffusion and mesh erosion), rather than factor-specific affinity, govern release, as also proposed by Schär et al. [48]; however, because fibrin degradation was not measured directly, this relationship remains hypothetical. An exploratory, descriptive cross-domain observation was consistent with this—higher porosity (>70%) samples tended to have a steeper early release slope between day 1 and day 3. In contrast, more densely meshed samples with higher G' had flatter early slopes, indicating that the early slope was not independent of either the architectural or the rheological properties measured here, but was indeed more strongly associated with the porosity. This relationship between structure and function reinforces the usefulness of multi-domain characterisation rather than relying on a single parameter reporting and may provide a rationale, to be tested in larger studies, for tuning the centrifugation parameters when a specific release profile is desired.

It should be emphasised that release was assessed in PBS at 37 °C, an enzyme-free and cell-free medium in which fibrin dissolution occurs mainly through passive diffusion, mechanical disintegration and non-enzymatic hydrolytic erosion. In vivo, fibrinolysis is driven enzymatically by plasmin (generated through tissue-type and urokinase-type plasminogen activators), by matrix metalloproteinases and other proteases released by infiltrating neutrophils and macrophages, and by cellular turnover [41]. These processes, together with tissue fluid exchange and binding of factors to the extracellular matrix and cell receptors, are likely to accelerate fibrin degradation and modify factor release and consumption. Consequently, the 14-day release profile observed here probably overestimates the in vivo residence time and should be regarded as a relative, protocol-specific in vitro descriptor rather than a direct predictor of in vivo kinetics.

There are a number of implications to the practical side of this. First, once confirmed in larger and more diverse cohorts, the preliminary reference distributions reported herein could be used to assess the quality of the preparations made in laboratories using i-PRF, so that the centrifugation drift, donor disease and/or sample manipulation can be quickly identified and the preparation rejected if it is out of the prescribed specification. Second, the consistent rheological signature may allow the generation of a "fingerprint" of injectability that is measurable and becomes more and more relevant with the introduction of the advanced therapy medicinal product classification by regulatory authorities for autologous platelet concentrates [49]. Third, the reproducibility observed under this single protocol, if confirmed across centres, could improve the credibility of the comparisons in multicentre

trials that have been used, in the past, to assess efficacy but that have been confounded by between-centre variability [50].

Translationally, the integrated fingerprint described here provides guidance and knowledge to guide the rational design of combination therapies involving i-PRF. The soft viscoelastic profile ($G' \approx 133$ Pa, $\tan \delta \approx 0.19$) places i-PRF in the mechanical range of native granulation tissue and dermis, suggesting that it can serve as a vehicle for biologics, micrografted cells, or particulate biomaterials without disturbing the cellular niche. The 14-day window corresponds to the time of the most metabolically active portion of the wound healing process—the proliferative phase—suggesting that a single i-PRF application could potentially provide matrix support during this period, although this was not tested in vivo. However, the present in vitro data cannot be used to define clinical re-injection intervals; the optimal dosing frequency for intra-articular or intradermal use must be established in in vivo pharmacokinetic and clinical studies.

Compared with conventional PRP, the main potential advantages suggested by this profile are threefold. First, i-PRF is prepared without anticoagulants or exogenous activators (thrombin or calcium chloride), allowing physiological, spontaneous polymerisation. Second, i-PRF converts in situ into a soft, predominantly elastic fibrin network ($G' \approx 133$ Pa, $\tan \delta \approx 0.19$) within approximately 7–9 min, which may help retain the injected product and its cellular and protein cargo at the target site, whereas liquid PRP may disperse more readily. Third, growth factors were released progressively over 14 days in vitro rather than predominantly within the first hours, as typically reported for activated PRP [6,7]. Whether these differences translate into superior clinical outcomes was not assessed in this study and requires head-to-head in vivo and clinical comparisons.

Limitations: The present data cannot be extrapolated to elderly, female-only or pathological populations without confirmation, due to the small and homogenous nature of the donor cohort (ten healthy adults aged 26–42 years, without a formal sample-size calculation); accordingly, all reference values and reproducibility estimates reported here should be considered preliminary and specific to the present centrifuge, tube and protocol. The processing variation due to the centrifuge or tube was not assessed because it was done at a single centre. The release kinetics were determined in enzyme-free PBS and not in physiological tissues or enzyme-containing media (e.g., plasmin- or MMP-supplemented buffers or serum-containing medium), so the enzymatic fibrinolysis that occurs in vivo was not reproduced, and fibrin degradation (e.g., clot mass loss or fibrin degradation products) was not measured in parallel with factor release; and the activity of the factors over longer time periods (>14 days) was not investigated. Although SEM allows for high-resolution snapshots of fibrin architecture, dynamic remodelling in the presence of cell load has not been captured, so complementary cryo-SEM or confocal fluorescence microscopy is recommended for future studies [51,52]. Leukocyte subsets were characterised only at the level of major classes, without assessment of activation or functional phenotype. Most importantly, the biological activities discussed in this study (e.g., anti-inflammatory, angiogenic and osteogenic potential) are inferred from protein concentrations alone and require confirmation with functional bioactivity assays, such as assays of fibroblast and endothelial cell migration, osteoblast differentiation, and macrophage polarisation to different effects from i-PRF supernatants. Lastly, a head-to-head comparison of i-PRF with other available platelet-concentrate protocols such as L-PRF and A-PRF, in the same donor population, is required to better place i-PRF in the broader spectrum of platelet-concentrate protocols.

5. Conclusions

PRF obtained from the Low-Speed Centrifugation Concept is an injectable autologous biologic that, in this preliminary single-centre study, showed consistent cellular, biochemi-

cal, ultrastructural, kinetic and viscoelastic parameters. The integrated reference dataset described herein (from 10 healthy donors with 8 pre-defined characterisation parameters) supports, at a compositional level, the ability of i-PRF to be platelet and leukocyte enriched, to contain a growth-factor and chemokine profile compatible with regeneration, to have a soft and porous fibrin structure, and to release growth factors over 14 days in vitro. The data offer preliminary, protocol-specific quantitative reference values for i-PRF preparation, which can be used to compare i-PRF preparations between centres, to support quality-control assessment and to guide design of comparative clinical and translational studies in the field of regenerative medicine. Confirmation in larger and more diverse donor cohorts, across different centrifuge and tube systems, and with functional bioactivity assays is required.

Supplementary Materials: The following supporting information can be downloaded at: https://www.mdpi.com/article/10.3390/biologics6040037/s1. Table S1: Cumulative growth-factor release over 14 days (long format).

Author Contributions: Conceptualization, P.R.P., A.M., M.J. and P.G.; methodology, P.R.P., N.J., A.N. and S.M.; software, R.V., S.M. and P.G.; validation, A.N., R.V. and S.M.; formal analysis, A.M., N.J., S.N.S.R., P.G. and M.J.; investigation, P.R.P., A.M., N.J. and M.J.; resources, N.J., R.V., S.M. and M.J.; data curation, P.R.P., A.M., A.N., S.N.S.R. and P.G.; writing—original draft preparation, N.J., A.N. and M.J.; writing—review and editing, A.N. and M.J.; visualization, A.N. and R.V.; supervision, M.J.; and project administration, M.J. All authors have read and agreed to the published version of the manuscript.

Funding: This research received no external funding.

Institutional Review Board Statement: The study was conducted in accordance with the Declaration of Helsinki, and approved by the Institutional Ethics Committee, Government Medical College, Omandurar Government Estate, Chennai (protocol code P-07/10/2025) on 29 October 2025.

Informed Consent Statement: Informed consent was obtained from all subjects involved in the study.

Data Availability Statement: The original contributions presented in this study are included in the article/Supplementary Material. Further inquiries can be directed to the corresponding author.

Conflicts of Interest: The authors declare no conflicts of interest.

References

1. Anitua, E.; Sánchez, M.; Orive, G.; Andía, I. The potential impact of the preparation rich in growth factors (PRGF) in different medical fields. *Biomaterials* **2007**, *28*, 4551–4560. [CrossRef] [PubMed]
2. Marx, R.E. Platelet-rich plasma (PRP): What is PRP and what is not PRP? *Implant Dent.* **2001**, *10*, 225–228. [CrossRef] [PubMed]
3. Choukroun, J.; Adda, F.; Schoeffler, C.; Vervelle, A. Une opportunité en paro-implantologie: Le PRF. *Implantodontie* **2001**, *42*, 55–62.
4. Dohan, D.M.; Choukroun, J.; Diss, A.; Dohan, S.L.; Dohan, A.J.; Mouhyi, J.; Gogly, B. Platelet-rich fibrin (PRF): A second-generation platelet concentrate. Part I: Technological concepts and evolution. *Oral Surg. Oral Med. Oral Pathol. Oral Radiol. Endodontology* **2006**, *101*, e37–e44. [CrossRef] [PubMed]
5. Ghanaati, S.; Booms, P.; Orlowska, A.; Kubesch, A.; Lorenz, J.; Rutkowski, J.; Landes, C.; Sader, R.; Kirkpatrick, C.; Choukroun, J. Advanced platelet-rich fibrin: A new concept for cell-based tissue engineering by means of inflammatory cells. *J. Oral Implantol.* **2014**, *40*, 679–689. [CrossRef] [PubMed]
6. Miron, R.J.; Fujioka-Kobayashi, M.; Hernandez, M.; Kandalam, U.; Zhang, Y.; Ghanaati, S.; Choukroun, J. Injectable platelet rich fibrin (i-PRF): Opportunities in regenerative dentistry? *Clin. Oral Investig.* **2017**, *21*, 2619–2627. [CrossRef] [PubMed]
7. Kobayashi, E.; Flückiger, L.; Fujioka-Kobayashi, M.; Sawada, K.; Sculean, A.; Schaller, B.; Miron, R.J. Comparative release of growth factors from PRP, PRF, and advanced-PRF. *Clin. Oral Investig.* **2016**, *20*, 2353–2360. [CrossRef] [PubMed]
8. Fujioka-Kobayashi, M.; Miron, R.J.; Hernandez, M.; Kandalam, U.; Zhang, Y.; Choukroun, J. Optimized platelet-rich fibrin with the low-speed concept: Growth factor release, biocompatibility, and cellular response. *J. Periodontol.* **2017**, *88*, 112–121. [CrossRef] [PubMed]

9. Ehrenfest, D.M.D.; Pinto, N.R.; Pereda, A.; Jiménez, P.; Del Corso, M.; Kang, B.-S.; Nally, M.; Lanata, N.; Wang, H.-L.; Quirynen, M. The impact of the centrifuge characteristics and centrifugation protocols on the cells, growth factors, and fibrin architecture of a leukocyte- and platelet-rich fibrin (L-PRF) clot and membrane. *Platelets* **2018**, *29*, 171–184. [CrossRef] [PubMed]
10. Wend, S.; Kubesch, A.; Orlowska, A.; Al-Maawi, S.; Zender, N.; Dias, A.; Miron, R.J.; Sader, R.; Booms, P.; Kirkpatrick, C.J.; et al. Reduction of the relative centrifugal force influences cell number and growth factor release within injectable PRF-based matrices. *J. Mater. Sci. Mater. Med.* **2017**, *28*, 188. [CrossRef] [PubMed]
11. Varela, H.A.; Souza, J.C.M.; Nascimento, R.M.; Araújo, R.F.; Vasconcelos, R.C.; Cavalcante, R.S.; Guedes, P.M.; Araújo, A.A. Injectable platelet rich fibrin: Cell content, morphological, and protein characterization. *Clin. Oral Investig.* **2019**, *23*, 1309–1318. [CrossRef] [PubMed]
12. Miron, R.J.; Zucchelli, G.; Pikos, M.A.; Salama, M.; Lee, S.; Guillemette, V.; Fujioka-Kobayashi, M.; Bishara, M.; Zhang, Y.; Wang, H.-L.; et al. Use of platelet-rich fibrin in regenerative dentistry: A systematic review. *Clin. Oral Investig.* **2017**, *21*, 1913–1927. [CrossRef] [PubMed]
13. Castro, A.B.; Meschi, N.; Temmerman, A.; Pinto, N.; Lambrechts, P.; Teughels, W.; Quirynen, M. Regenerative potential of leucocyte- and platelet-rich fibrin. Part A: Intra-bony defects, furcation defects and periodontal plastic surgery. *J. Clin. Periodontol.* **2017**, *44*, 67–82. [CrossRef] [PubMed]
14. Strauss, F.J.; Stähli, A.; Gruber, R. The use of platelet-rich fibrin to enhance the outcomes of implant therapy: A systematic review. *Clin. Oral Implant. Res.* **2018**, *18*, 6–19. [CrossRef] [PubMed]
15. Hassan, H.; Quinlan, D.J.; Ghanem, A. Injectable platelet-rich fibrin for facial rejuvenation: A prospective, single-center study. *J. Cosmet. Dermatol.* **2020**, *19*, 3213–3221. [CrossRef] [PubMed]
16. Mohale, S.A.; Thakare, P.V.; Gaurkar, S.S.; Bharadia, G.; Acharya, S. Effectiveness of Injectable Platelet-Rich Fibrin Therapy in Alopecia and Facial Rejuvenation: A Systematic Review. *Cureus* **2024**, *16*, e62198. [CrossRef] [PubMed]
17. Panni, A.S.; Vasso, M.; Braile, A.; Toro, G.; De Cicco, A.; Viggiano, D.; Lepore, F. Preliminary results of autologous adipose-derived stem cells in early knee osteoarthritis: Identification of a subpopulation with greater response. *Int. Orthop.* **2019**, *43*, 7–13. [CrossRef] [PubMed]
18. Jeyaraman, M. Comparative Efficacy of Leukocyte-Poor Platelet-Rich Plasma, Leukocyte-Rich Platelet-Rich Plasma, Injectable Platelet-Rich Fibrin, and Corticosteroid Injections in Kellgren–Lawrence Grade 2–3 Knee Osteoarthritis: A Prospective Comparative Study. *J. Orthop. Case Rep.* **2026**, *16*, 330–338. [CrossRef] [PubMed]
19. Everts, P.A.; Knape, J.T.; Weibrich, G.; Schönberger, J.P.; Hoffmann, J.; Overdevest, E.P.; Box, H.A.; van Zundert, A. Platelet-rich plasma and platelet gel: A review. *J. Extracorpor. Technol.* **2006**, *38*, 174–187. [CrossRef]
20. Pinto, N.R.; Ubilla, M.; Zamora, Y.; Del Río, V.; Dohan Ehrenfest, D.M.; Quirynen, M. Leucocyte- and platelet-rich fibrin (L-PRF) as a regenerative medicine strategy for the treatment of refractory leg ulcers: A prospective cohort study. *Platelets* **2018**, *29*, 468–475. [CrossRef] [PubMed]
21. Schär, M.O.; Diaz-Romero, J.; Kohl, S.; Zumstein, M.A.; Nesic, D. Platelet-rich concentrates differentially release growth factors and induce cell migration in vitro. *Clin. Orthop. Relat. Res.* **2015**, *473*, 1635–1643. [CrossRef] [PubMed]
22. Lourenço, E.S.; Mourão, C.F.A.B.; Leite, P.E.C.; Granjeiro, J.M.; Calasans-Maia, M.D.; Alves, G.G. The in vitro release of cytokines and growth factors from fibrin membranes produced through horizontal centrifugation. *J. Biomed. Mater. Res. A* **2018**, *106*, 1373–1380. [CrossRef] [PubMed]
23. Madurantakam, P.; Yoganarasimha, S.; Hasan, F.K. Characterization of leukocyte-platelet rich fibrin, a novel biomaterial. *J. Vis. Exp.* **2015**, *103*, e53221. [CrossRef] [PubMed]
24. Pavlovic, V.; Ciric, M.; Jovanovic, V.; Trandafilovic, M.; Stojanovic, P. Platelet-rich fibrin: Basics of biological actions and protocol modifications. *Open Med.* **2021**, *16*, 446–454. [CrossRef] [PubMed]
25. Steller, D.; Herbst, N.; Pries, R.; Juhl, D.; Hakim, S.G. Positive impact of platelet-rich plasma and platelet-rich fibrin on viability, migration and proliferation of osteoblasts and fibroblasts treated with zoledronic acid. *Sci. Rep.* **2019**, *9*, 8310. [CrossRef] [PubMed]
26. Ravi, S.; Santhanakrishnan, M. Mechanical, chemical, structural analysis and comparative release of PDGF-AA from L-PRF, A-PRF and T-PRF—An in vitro study. *Biomater. Res.* **2020**, *24*, 16. [CrossRef] [PubMed]
27. El Bagdadi, K.; Kubesch, A.; Yu, X.; Al-Maawi, S.; Orlowska, A.; Dias, A.; Booms, P.; Dohle, E.; Sader, R.; Kirkpatrick, C.J.; et al. Reduction of relative centrifugal forces increases growth factor release within solid platelet-rich-fibrin (PRF)-based matrices: A proof-of-concept of LSCC. *Eur. J. Trauma Emerg. Surg.* **2019**, *45*, 467–479. [CrossRef] [PubMed]
28. Ghanaati, S.; Al-Maawi, S.; Conrad, T.; Lorenz, J.; Rössler, R.; Sader, R. Biomaterial-based bone regeneration and soft tissue management of the individualized 3D-titanium mesh: An alternative concept to autologous transplantation and flap mobilization. *J. Craniomaxillofac. Surg.* **2019**, *47*, 1633–1644. [CrossRef] [PubMed]

29. Choukroun, J.; Ghanaati, S. Reduction of relative centrifugation force within injectable platelet-rich-fibrin (PRF) concentrates advances patients' own inflammatory cells, platelets and growth factors: The first introduction to the low speed centrifugation concept. *Eur. J. Trauma Emerg. Surg.* **2018**, *44*, 87–95. [CrossRef] [PubMed]
30. Tsujino, T.; Masuki, H.; Nakamura, M.; Isobe, K.; Kawabata, H.; Aizawa, H.; Watanabe, T.; Kitamura, Y.; Okudera, H.; Okuda, K.; et al. Striking differences in platelet distribution between advanced-platelet-rich fibrin and concentrated growth factors: Effects of silica-containing plastic tubes. *J. Funct. Biomater.* **2019**, *10*, 43. [CrossRef] [PubMed]
31. Kubesch, A.; Barbeck, M.; Al-Maawi, S.; Orlowska, A.; Booms, P.F.; Sader, R.A.; Miron, R.J.; Kirkpatrick, C.J.; Choukroun, J.; Ghanaati, S. A low-speed centrifugation concept leads to cell accumulation and vascularization of solid platelet-rich fibrin: An experimental study in vivo. *Platelets* **2019**, *30*, 329–340. [CrossRef] [PubMed]
32. Miron, R.J.; Pinto, N.R.; Quirynen, M.; Ghanaati, S. Standardization of relative centrifugal forces in studies related to platelet-rich fibrin. *J. Periodontol.* **2019**, *90*, 817–820. [CrossRef] [PubMed]
33. Miron, R.J.; Chai, J.; Zheng, S.; Feng, M.; Sculean, A.; Zhang, Y. A novel method for evaluating and quantifying cell types in platelet rich fibrin and an introduction to horizontal centrifugation. *J. Biomed. Mater. Res. A* **2019**, *107*, 2257–2271. [CrossRef] [PubMed]
34. Ehrenfest, D.M.D.; Andia, I.; Zumstein, M.A.; Zhang, C.Q.; Pinto, N.R.; Bielecki, T. Classification of platelet concentrates (Platelet-Rich Plasma-PRP, Platelet-Rich Fibrin-PRF) for topical and infiltrative use in orthopedic and sports medicine: Current consensus, clinical implications and perspectives. *Muscles Ligaments Tendons J.* **2014**, *4*, 3–9. [CrossRef]
35. Ehrenfest, D.M.D.; Del Corso, M.; Diss, A.; Mouhyi, J.; Charrier, J. Three-dimensional architecture and cell composition of a Choukroun's platelet-rich fibrin clot and membrane. *J. Periodontol.* **2010**, *81*, 546–555. [CrossRef] [PubMed]
36. Bielecki, T.; Dohan Ehrenfest, D.M.; Everts, P.A.; Wiczkowski, A. The role of leukocytes from L-PRP/L-PRF in wound healing and immune defense: New perspectives. *Curr. Pharm. Biotechnol.* **2012**, *13*, 1153–1162. [CrossRef] [PubMed]
37. Wang, X.; Guan, Y.; Xiang, S.; Clark, K.L.; Alexander, P.G.; Simonian, L.E.; Deng, Y.; Lin, H. Role of Canonical Wnt/β-Catenin Pathway in Regulating Chondrocytic Hypertrophy in Mesenchymal Stem Cell-Based Cartilage Tissue Engineering. *Front. Cell Dev. Biol.* **2022**, *10*, 812081. [CrossRef] [PubMed]
38. Karimi, K.; Rockwell, H. The benefits of platelet-rich fibrin. *Facial Plast. Surg. Clin. N. Am.* **2019**, *27*, 331–340. [CrossRef] [PubMed]
39. Anitua, E.; Pino, A.; Orive, G. Plasma rich in growth factors promotes dermal fibroblast proliferation, migration and biosynthetic activity. *J. Wound Care* **2016**, *25*, 680–687. [CrossRef] [PubMed]
40. Marx, D.R.E.; Carlson, D.E.R.; Eichstaedt, D.R.M.; Schimmele, D.S.R.; Strauss, D.J.E.; Georgeff, K.R. Platelet-rich plasma: Growth factor enhancement for bone grafts. *Oral Surg. Oral Med. Oral Pathol. Oral Radiol. Endodontology* **1998**, *85*, 638–646.
41. Mosesson, M.W. Fibrinogen and fibrin structure and functions. *J. Thromb. Haemost.* **2005**, *3*, 1894–1904. [CrossRef] [PubMed]
42. Kim, T.H.; Kim, S.H.; Sándor, G.K.; Kim, Y.D. Comparison of platelet-rich plasma (PRP), platelet-rich fibrin (PRF), and concentrated growth factor (CGF) in rabbit-skull defect healing. *Arch. Oral Biol.* **2014**, *59*, 550–558. [CrossRef] [PubMed]
43. Karde, P.A.; Sethi, K.S.; Mahale, S.A.; Khedkar, S.U.; Patil, A.G.; Joshi, C.P. Comparative evaluation of platelet count and antimicrobial efficacy of injectable platelet-rich fibrin with other platelet concentrates: An in vitro study. *J. Indian Soc. Periodontol.* **2017**, *21*, 97–101. [CrossRef] [PubMed]
44. Khorshidi, H.; Raoofi, S.; Bagheri, R.; Banihashemi, H. Comparison of the mechanical properties of early leukocyte- and platelet-rich fibrin versus PRGF/Endoret membranes. *Int. J. Dent.* **2016**, *2016*, 1849207. [CrossRef] [PubMed]
45. Isobe, K.; Watanebe, T.; Kawabata, H.; Kitamura, Y.; Okudera, T.; Okudera, H.; Uematsu, K.; Okuda, K.; Nakata, K.; Tanaka, T.; et al. Mechanical and degradation properties of advanced platelet-rich fibrin (A-PRF), concentrated growth factors (CGF), and platelet-poor plasma-derived fibrin (PPTF). *Int. J. Implant Dent.* **2017**, *3*, 17. [CrossRef] [PubMed]
46. Pitzurra, L.; Jansen, I.D.C.; Vries, T.J.; Hoogenkamp, M.A.; Loos, B.G. Effects of L-PRF and A-PRF+ on periodontal fibroblasts in in vitro wound healing experiments. *J. Periodontal Res.* **2020**, *55*, 287–295. [CrossRef] [PubMed]
47. Fujioka-Kobayashi, M.; Schaller, B.; Mourão, C.F.A.B.; Zhang, Y.; Sculean, A.; Miron, R.J. Biological characterization of an injectable platelet-rich fibrin mixture consisting of autologous albumin gel and liquid platelet-rich fibrin (Alb-PRF). *Platelets* **2021**, *32*, 74–81. [CrossRef] [PubMed]
48. Kobayashi, M.; Kawase, T.; Horimizu, M.; Okuda, K.; Wolff, L.F.; Yoshie, H. A proposed protocol for the standardized preparation of PRF membranes for clinical use. *Biologicals* **2012**, *40*, 323–329. [CrossRef] [PubMed]
49. Miron, R.J.; Xu, H.; Chai, J.; Wang, J.; Zheng, S.; Feng, M. Comparison of platelet, leukocyte, and growth factor levels in point-of-care platelet-enriched plasma, advanced platelet-rich fibrin, and concentrated growth factor. *Clin. Oral Investig.* **2020**, *24*, 1939–1947.
50. Burnouf, T.; Strunk, D.; Koh, M.B.C.; Schallmoser, K. Human platelet lysate: Replacing fetal bovine serum as a gold standard for human cell propagation? *Biomaterials* **2016**, *76*, 371–387. [CrossRef] [PubMed]

51. Dragonas, P.; Katsaros, T.; Avila-Ortiz, G.; Chambrone, L.; Schiavo, J.H.; Palaiologou, A. Effects of leukocyte–platelet-rich fibrin (L-PRF) in different intraoral bone grafting procedures: A systematic review. *Int. J. Oral Maxillofac. Surg.* **2019**, *48*, 250–262. [CrossRef] [PubMed]
52. Quirynen, M.; Blanco, J.; Wang, H.L.; Donos, N.; Temmerman, A.; Castro, A.; Pinto, N. Instructions for the use of L-PRF in different clinical indications. *Periodontol. 2000* **2025**, *97*, 420–432. [CrossRef] [PubMed]

Disclaimer/Publisher's Note: The statements, opinions and data contained in all publications are solely those of the individual author(s) and contributor(s) and not of MDPI and/or the editor(s). MDPI and/or the editor(s) disclaim responsibility for any injury to people or property resulting from any ideas, methods, instructions or products referred to in the content.